

Effective Biosorption of Auramin O Dye with Sustainable Chickpea Pods Waste; Isotherms, Kinetics and Thermodynamic Analysis

Zehra Saba Keskin^{1,a,*}

¹ Department of Pharmacy, Cumhuriyet University, Health Services Vocational School, Sivas 58140, Türkiye.

*Corresponding author

Research Article

History

Received: 22/03/2024

Accepted: 14/06/2024



This article is licensed under a Creative Commons Attribution-NonCommercial 4.0 International License (CC BY-NC 4.0)

ABSTRACT

This study investigated biosorbent properties in removing Auramin O (AO) dye from the aqueous solution of agricultural wastes released from chickpea (*Cicer arietinum* L.), which is widely produced in Turkey and the world. Biosorption studies were carried out using different values of parameters such as initial AO concentration, dye pH, contact time, temperature, and biosorbent amount. Characterization analyses of the biosorbent used before and after biosorption were carried out by scanning electron microscopy (SEM), energy dispersive X-ray (EDX), Brunauer–Emmett–Teller (BET), Fourier transform infrared spectroscopy (FTIR), and point of zero charge (PZC). Biosorption isotherms were evaluated using Langmuir, Freundlich, and Dubinin-Radushkevich (D-R) isotherm models. As a result of experimental data, it has been shown that the Langmuir isotherm model ($R^2 = 0.930$) is the most compatible model for biosorption, while the biosorption kinetic mechanism proceeds through the pseudo-second-order (PSO) kinetic model ($R^2 = 0.965$) and the intra-particle diffusion model. As a result of thermodynamic studies, it has been reported that biosorption is endothermic ($\Delta H > 0$), spontaneous ($\Delta S > 0$), and entropy-increasing ($\Delta G < 0$).

Keywords: *Cicer arietinum* L. pods, Auramin O, Biosorption.

^a zkeskin@cumhuriyet.edu.tr

^{ID} <https://orcid.org/0000-0003-1334-5158>

Introduction

All living organisms require high-quality water to sustain their lives in a healthy way. However, due to demographic growth, wastewaters resulting from increasing anthropogenic activities are discharged directly into water bodies [1]. Synthetic dyes are among the pollutants that cause high water pollution levels.

Due to being low-cost, brightly coloured, and highly stable against environmental conditions, dyes are widely used in various industries such as textiles, paper, pharmaceuticals, food, plastic coating, and cosmetics [2]. However, discharging wastewater contaminated with dyes without any treatment poses a great danger in terms of aesthetics and the harm it causes to the ecosystem.

According to the United Nations World Water Assessment Programme report for 2023, water sources receive a daily discharge of 2 tonnes of wastewater [3].

The presence of dyes in water ecosystems leads to a decrease in light penetration, an increase in chemical oxygen demand, and toxicity for living organisms in the water. Furthermore, it causes respiratory disorders, skin irritation, burns, allergic reactions, cancer, and mutations in human health [4].

Auramine O (AO) dye, also referred to as Basic Yellow 2, is an easily soluble yellow cationic dye used as a colorant in various industries such as textile, ink, leather, and paper. The International Agency for Research on Cancer (IARC) has classified AO as a carcinogenic chemical. Therefore, it is crucial to purify wastewater using various methods and dispose of it in natural ecosystems. Several studies have been conducted in recent years using methods such as coagulation, photodegradation, membrane filtration, ion exchange, ozonation, solvent extraction, hyperfiltration adsorption (biosorption) [3].

The adsorption method has gained attention due to its simplicity, cost-effectiveness, environmental friendliness, high efficiency, and absence of harmful by-products.

However, the high performance and efficiency of the adsorption method also depend on the morphological characteristics of the preferred adsorbent, and whether it is edible, cheap, and abundant. Recently, agricultural wastes have been seen as an alternative to traditional adsorbents. Most agricultural wastes are lignocellulosic in structure and contain functional compounds such as hydroxyl, amine, aldehyde, ketone, and phenol. The presence of these functional compounds, which can bind dyes, and their porous and loose structures increase the effectiveness of agricultural wastes in purifying dyes from wastewater [5,6]. In addition, utilizing waste from agriculture as a biosorbent will help climate neutrality with a sustainable product strategy [7].

Therefore, in recent years, researchers have conducted studies on removing dyes using agricultural waste as an alternative to traditional adsorbents. Examples of such waste include potato peel [8], wheat straw (*T. aestivum*) [9], jackfruit leaves [3], corn husk waste [10], rosemary waste [11], and Alfa (*Stipa tenacissima* L.) leaf powder [12].

Chickpeas (*Cicer arietinum* L.) belong to the Viceae genus of the *Leguminosae* family and are originally from West Asia and Near East Asia [13]. They are one of the most widely produced legumes globally and in Turkey, making them a crucial component of the Turkish economy. However, a significant amount of agricultural waste generated from this production is either burned or left untreated in the environment. Therefore, using these

wastes as biosorbents could yield ecological, economic, and social benefits.


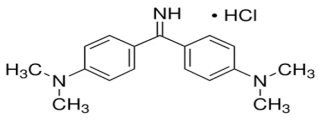
This study examines the potential use of chickpea peels (CPP) as biosorbents for the removal of AO from aqueous solutions. This report presents the first study on the use of chickpea outer husks as a biosorbent for removing AO dye. We conducted characterization analyses on the unmodified biosorbent before and after biosorption and examined the effects of parameters such as pH, initial dye concentration, time, temperature, and biosorbent amount on the biosorption process.

Materials and Methods

Chemicals

Chemicals with analytical purity were used in the experiment. The AO dye (powder form) (Table 1), KNO₃, HCl, and NaOH used in the experiment were purchased from Merck. All analyses were conducted using double-distilled water.

Table 1. Properties of Auamine O

Physicochemical	Values
Chemicals formula	C ₁₇ H ₂₁ N ₃ · HCl
Molecule weight (g/mol)	303.83
Class	Cationic dye
λ _{max} (nm)	434
Molecular structure	
	

Characterization and Preparation of CPP

CPP was obtained from chickpeas harvested in the Kangal region of Sivas. The CPP was subjected to a distilled water washing process to remove any physical impurities. It was then dried in the oven at 50°C for 24 hours. To increase the surface area of the biosorbent, it was crushed with an IKA A 11 grinder. The prepared CPP biosorbent was stored in airtight propylene containers until further processing.

The equilibrium solution concentrations of AO were determined by analyzing absorbance values at 434 nm using a UV-Vis spectrophotometer (Peak, E 1000). Functional compound analysis of CPP before and after AO biosorption was conducted using FTIR spectroscopy (ATR, Bruker, Tensor II). Additionally, changes in surface morphology and elemental composition before and after biosorption were assessed using Energy Dispersive X-ray spectroscopy (EDX) coupled with a Scanning Electron Microscope (Tescan Mira3 XMU). Samples were coated with gold in an automatic coater before analysis to increase process surface conductivity and obtain better quality images. Additionally, the pH of the zero charge point (pHpzc) of CPP was determined using the solid addition method [14].

Biosorption Procedure

The batch method was used to examine the adsorptive efficiency of CPP in removing AO dye. A stock AO dye solution at a concentration of 1000 ppm was prepared by dissolving 1 g of dye in 1000 ml of distilled water. Different initial dye concentrations (10-1000 ppm) were created by diluting this stock solution at varying rates. To evaluate the biosorption process, experiments were conducted in a 10 ml volume of 500 ppm AO dye solution using 50 mg CPP at pH 6.2 at 298 K in a constantly shaking water bath for 24 hours. The equilibrium solutions were then filtered through the Whatman filter paper, and the non-adsorbed concentrations were calculated using linear regression equations based on the absorbance values read on the UV-Vis spectrophotometer.

Additionally, experiments were conducted with different values of parameters such as initial AO concentration (10-1000 ppm), dye pH (2-12), contact time (2-1440 min.), and temperature (5, 25, 40 °C) to determine the optimum conditions for biosorption.

Percentage of AO removal (%R), amount of AO adsorbed at equilibrium (Q, mg/g), and Recovery% were calculated using the following Equations [1-3], respectively [15].

$$\% R = \left(\frac{C_o - C_e}{C_o} \right) \times 100 \quad (1)$$

$$Q = (C_o - C_e) \cdot \frac{V}{m} \quad (2)$$

$$\text{Recovery}\% = \frac{Q_{des}}{Q_{ads}} \times 100 \quad (3)$$

Here, C_o (ppm) and C_e (ppm) are the initial and equilibrium concentrations of the AO dye, m (g) is the amount of adsorbent, and V (L) is the volume of the AO dye solution.

Results and Discussion

FTIR

FTIR analysis was conducted before and after biosorption to identify functional groups aiding in the biosorption process of AO dye molecules onto CPP. The FTIR spectra were obtained in the range of 4000-400 cm⁻¹ and are depicted in Figure 1.

The peak at 3307 cm⁻¹ observed in the range of 3680-3000 cm⁻¹ is attributed to the stretching vibration of the amine group (-NH₂) and the hydroxyl group (-OH) present in lignin, cellulose, and hemicellulose [16].

The small sharp peaks at 2920 and 2850 cm⁻¹ correspond to the symmetric and asymmetric C-H stretching of methoxy groups in lignocellulosic structures, while the peak at 1738 cm⁻¹ corresponds to the C=O stretching vibration of carboxylic acid [17].

The peak observed at 1623 cm⁻¹ corresponds to the C=O stretching of carboxylic acid groups, while the peak at 1425 cm⁻¹ is attributed to the C=C stretching in aromatic rings [18].

The sharp peak at 1021 cm⁻¹ indicates the presence of C-O and C-N bonds, which are characteristic of proteins, alcohols, and ethers. Additionally, it suggests the presence of lignin in CPP [16,17,19]. As seen in Figure 1, changes in

the intensity and positions of peaks in the FTIR spectrum have been observed due to the interactions between the functional groups and the AO dye molecules adhering to the biosorbent surface. The peaks at 1623 and 1021 cm^{-1} shifted to 1600 and 1006 cm^{-1} , respectively, and the intensity of all peaks decreased after biosorption. The changes observed before and after biosorption may be attributed to electrostatic interactions between functional groups and AO, as well as surface complexation reactions.

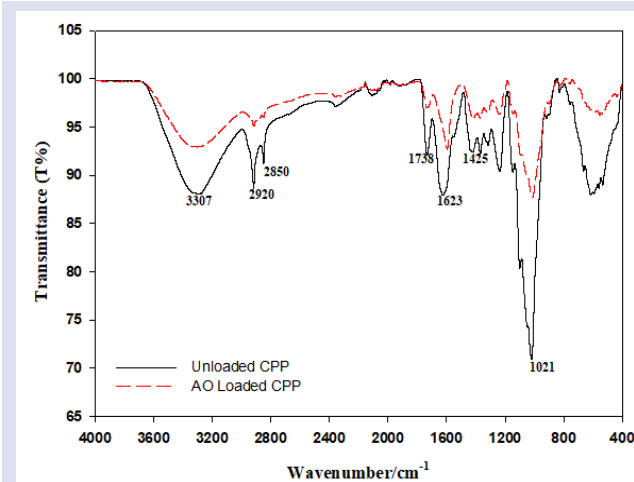


Figure 1. FTIR analysis of CPP pre- and post-AO biosorption in the panels. Error bars show \pm SD values.

SEM-EDX and BET Analyzes

SEM was used to examine the morphological characteristics and surface features of CPP biomass before (Figure 2a) and after (Figure 2b) the biosorption process.

The SEM images in Figure 2a show that the surface of the CPP biosorbent was smooth before the biosorption process. However, after the biosorption process, large dye particles were observed on the biosorbent, as shown in Figure 2b, indicating successful biosorption.



The EDX spectrum in Figures 3a and 3b shows the elemental composition on the CPP surface before and after biosorption, respectively. In the spectrum obtained before biosorption, C (51.7% by weight), O (47.3% by weight), Ca (0.6% by weight), Mg (0.2% by weight) and Al (0.2% by weight) its existence has been determined.

The appearance of new elements, especially nitrogen (9 wt%) and chlorine (0.2 wt%), and changes in composition in the EDX spectrum after biosorption indicate that the biosorption process has occurred. The detection of these elements, including carbon, hydrogen, nitrogen and chlorine atoms in the chemical composition of AO, in the spectrum can be shown as evidence that biosorption has occurred.

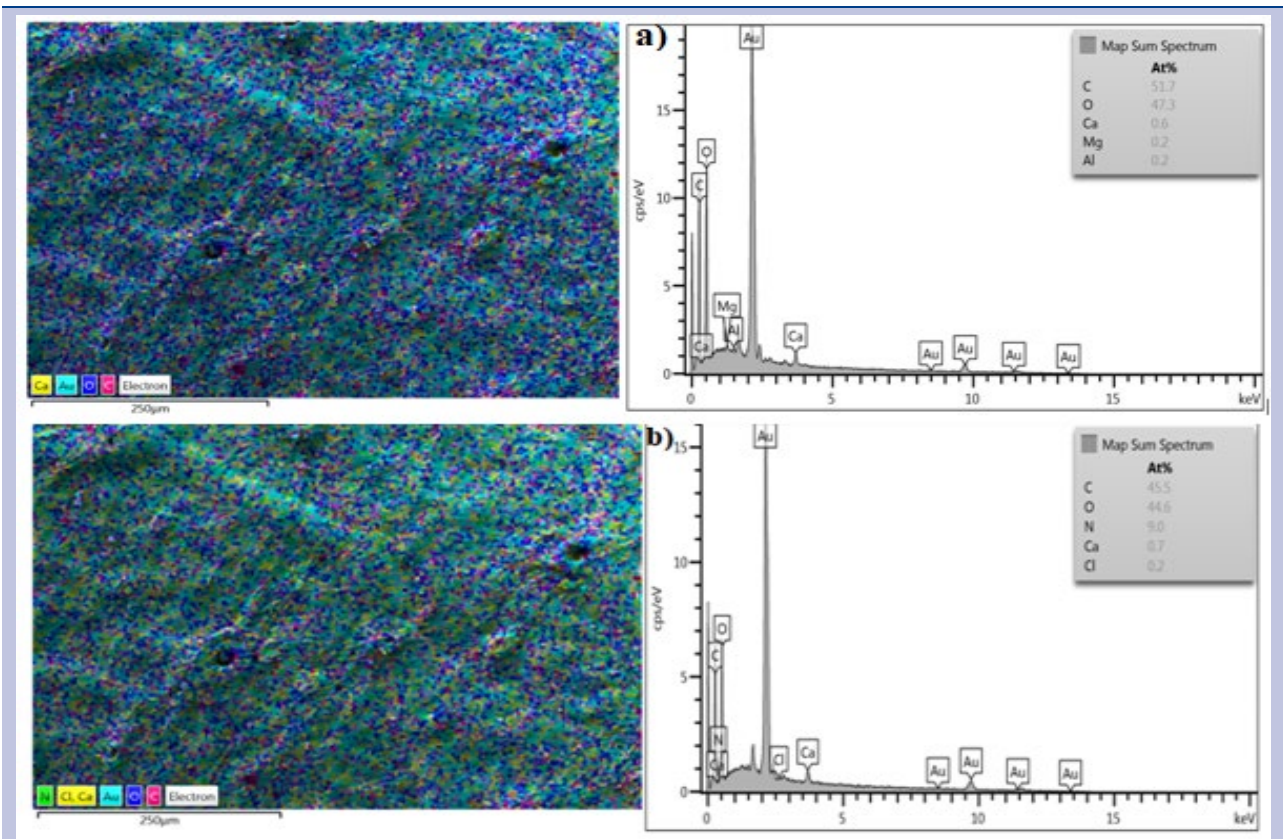


Figure 3. EDX spectra before (a) and after (b) AO biosorption

BET surface area ($\text{m}^2 \text{g}^{-1}$) analysis was performed for CPP biosorbent before and after biosorption. It was determined that the surface area of CPP before biosorption was $50,872 \text{ m}^2 \text{g}^{-1}$ and after biosorption, the surface area decreased to $31,460 \text{ m}^2 \text{g}^{-1}$. This apparent decrease in surface area can be attributed to the adhesion of AO dye molecules to the CPP pores.

Effect of PZC and pH on Biosorption

The pH of the dye is crucial in controlling the biosorption process as it impacts the surface structure of the biosorbent and alters the electrostatic interactions between the dye and the biosorbent [20].

To determine the effect of pH on the biosorption of AO dye onto CPP, experiments were carried out at different pH values ranging from 2-12, with a contact time of 1440 minutes and an amount of 50 mg biosorbent. The findings on the relationship between solution pH and biosorption capacity are presented in Figure 4.

The neutral pH value on the surface of the biosorbent plays a critical role in understanding the surface kinetics and biosorption mechanism. This value is also important in explaining the interaction of dye molecules with the biosorbent and the chemical structures of the active sites for the biosorption process. At $\text{pH} > \text{pH}_{\text{pzc}}$ values, the biosorbent surface carries a negative charge, while at $\text{pH} < \text{pH}_{\text{pzc}}$ values, the biosorbent surface carries a positive charge [21].

As depicted in Figure 5, the pH_{pzc} value of the CPP biosorbent was determined to be 4.91. Consequently, when the solution pH is below 4.91, the CPP surface is positively charged, whereas a solution pH above 4.91 indicates a negatively charged biosorbent surface. Hence, pH values exceeding the pH_{pzc} are conducive to the removal of AO, which is a cationic dye.

Based on the data obtained, as seen in Figure 4, a decrease in AO removal is observed between pH 2 and pH 4.

The decrease in RhB dye biosorption by CPP at low pH can be attributed to the competition between the cationic groups in the dye and the H^+ ions in the solution for the biosorption sites in the CPP. Additionally, electrostatic repulsion between the protonated surface of CPP and the cationic dye can be shown as another reason [22].

The interaction between AO and chickpea shell is found to increase between pH 4-6 and pH 8-12 compared to lower pH values due to the heightened electrostatic attraction forces between the increasingly negatively charged regions and the positively charged cationic dye. This strong binding facilitates the biosorption of AO onto the CPP biosorbent [23].

Although the removal amount was expected to increase between pH 6 and pH 8, a slight decrease was observed. This decrease can be attributed to the NaOH used in pH adjustment of AO dye solutions and the Cl in the structure of the AO dye entering into a substitution reaction that causes the formation of NaCl [24].

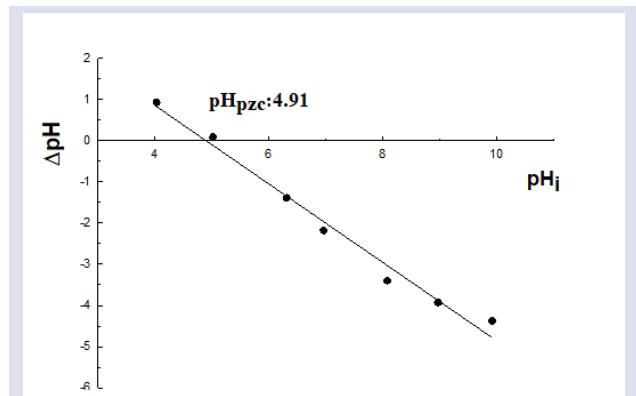


Figure 5. PZC plots of CPP biosorbent

Effect of CPP Amount on Biosorption

It is crucial to determine the optimal amount of biosorbent dose in order to achieve high biosorption efficiency and lower the cost of biosorbent. The experiment investigated the effect of different biosorbent doses (ranging from 5-20 g L^{-1}) on AO removal and its interpretation can be found in Figure 6.

The results show that as the biosorbent dose increased, the percentage of AO removal rate also increased. This is due to the increase in active biosorption sites and total surface area caused by the increase in biosorbent amount [25].

However, an increase in the biosorbent dose led to a decrease in the amount of biosorbed AO dye per unit. This is because the number of active sites was not sufficiently saturated by AO dye molecules. The highest biosorption capacity (53.03 mg g^{-1}) was obtained with an adsorbent dose of 5 g L^{-1} .

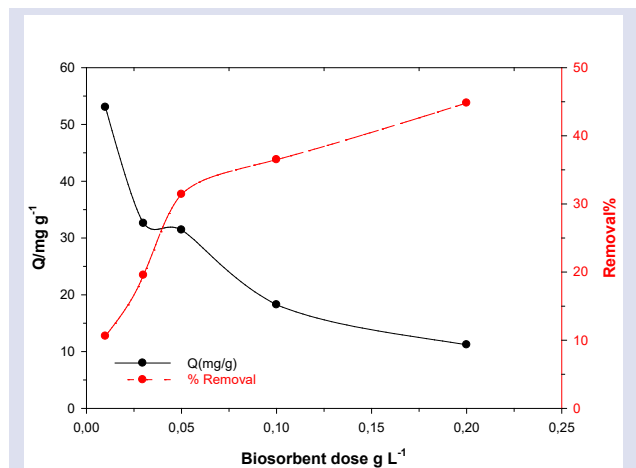


Figure 6. Effect of CPP amount on AO biosorption.

Biosorption Equilibrium Isotherm Modelling

Biosorption isotherms play a crucial role in interpreting the interaction between biosorbent and dye, explaining the biosorption mechanism, and determining the biosorption capacity of the biosorbent [26].

The investigation of AO dye molecule biosorption onto CPP involved the application of three isotherm models to the experimental data: Langmuir [27], Freundlich [28], and Dubinin-Radushkevich (D-R) [29]. Analyzes in which isotherm models were determined were carried out at

different initial concentrations of AO dye (10-1000 mg L⁻¹), 50 mg CPP, pH 6.2 and 1440 minutes contact time.

Table 2 presents the nonlinear equations for the Langmuir, Freundlich, and D-R isotherm models used in the removal of AO dye on CPP, along with the corresponding isotherm parameters.

The Langmuir isotherm model assumes biosorption occurs on monolayer homogeneous surfaces with equal energy of the biosorbent.

Although the Freundlich isotherm model assumes that biosorption occurs on reversible and multilayered heterogeneous surfaces, it also provides information about the adsorbent concentration adhering to the biosorbent.

The D-R isotherm model states that the adsorption potential on heterogeneous surfaces depends on the pore structure of the adsorbent. It also states that biosorption proceeds physically or chemically, evaluated in terms of energy.

The equilibrium of biosorption of AO dye molecules is observed at a concentration of 500 mg L⁻¹, as shown in Figure 7. The suitability of isotherm models for the biosorption process was assessed by comparing the correlation coefficients (R²).

When comparing the R² values of isotherm models, it was determined that the equilibrium data was more compatible with the Langmuir model, which describes single-layer biosorption with an R² value close to 1. According to the Langmuir isotherm, the maximum biosorption capacity (q_m) of CPP biosorbent is 177.96 mg/g. The Langmuir equilibrium constant (K_L), which is related to the appropriate surface area and porosity of the biosorbent, was calculated as 6.596 x10⁻⁴. This parameter describes the binding of AO molecules in a single layer on homogeneous CPP surfaces.

The Freundlich constant (K_f) that determines the biosorption capacity and the β value that indicates surface heterogeneity intensity were determined as 0.2486 L mg⁻¹

and 0.831, respectively. The β value within the range of 0 < β < 1 indicates the suitability of biosorption of AO dye molecules onto CPP [30].

D-R isotherm model aims to explain the biosorption process and pore filling mechanism by distributing Gauss energy across a non-uniform surface. The D-R isotherm model can be used to calculate the average biosorption free energy per biosorbent molecule (E) and determine whether the process is physical or chemical in nature [31]. The calculated E value of 7.128 kJ mol⁻¹ suggests that the interaction between AO dye and CPP surface occurred through physisorption, as it is less than 8 kJ mol⁻¹.

Table 3 presents a comparison of the maximum adsorption capacities of various adsorbents used for AO removal. The raw agricultural waste used in this study, without any modification, exhibited a higher maximum adsorption capacity than many other adsorbents. This suggests that CPP could be a cost-effective and readily available biosorbent with a high biosorption capacity for AO removal.

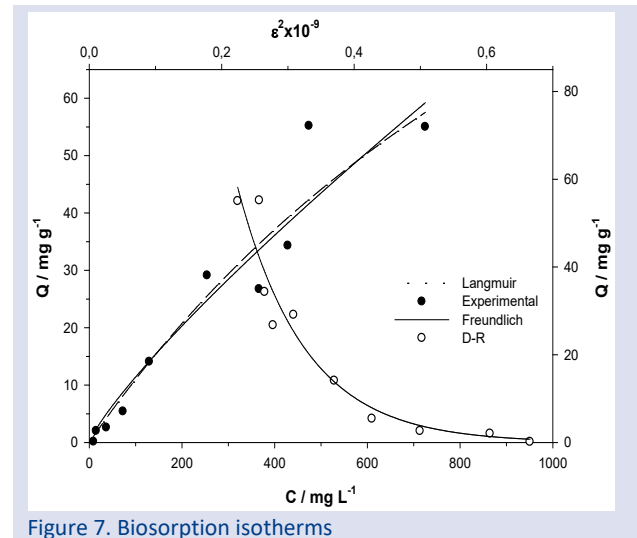


Figure 7. Biosorption isotherms

Table 2. Equations and parameters for nonlinear isotherm models

Isotherms	Equations	Parameters	Values	R ²
Langmuir	$Q = \frac{K_L \cdot q_m \cdot C_e}{1 + K_L \cdot C_e}$	q _m (mg/g) K _L (L/ mg)	177,96 6,596 x10 ⁻⁴	0,930
Freundlich	$Q = K_F \cdot C_e^\beta$	K _F β	2,486 x10 ⁻¹ 8,313 x10 ⁻¹	0,924
D-R	$Q = X_{DR} \cdot e^{-K_{DR} \cdot \epsilon^2}$ $\epsilon = R \cdot T \ln(1 + \frac{1}{C_e})$ $E = \frac{1}{\sqrt{2K_{DR}}}$	X _{DR} (mg/ g) K _{DR} (mol ² K/ J ²) E (kJ /mol)	5,278 x10 ⁻² 9,84 x10 ⁻⁹ 7,128	0,929

Table 3. Comparison of maximum adsorption capacities (qm) for the removal of AO by various adsorbents

Sorbents	T (°C)	pH	qm (mg/g)	References
Chickpea pods (CPP)	25	6.2	177,96	This study
Chitosan–kaolin composite	25	7.5	35,5	[32]
Activated jackfruit leaf powder	-	-	79,36	[3]
<i>Pyracantha Coccinea</i>	25	-	123,1	[33]
Kernel powder/kappa-carrageenan hydrogel	-	11	9,225	[34]
Fe3O4-based melamine-rich covalent organic polymer	-	-	107,11	[35]
Amazon raw clay	28	5,6	18.04	[36]

Biosorption Kinetic Modelling

In order to examine the kinetic mechanism of AO dye biosorption onto CPP, pseudo-first-order kinetic model (PFO) [37], pseudo-second-order kinetic model (PSO) [38], and intra-particle diffusion model (IPD) [27] were utilized.

The kinetic studies were conducted at varying time intervals ranging from 2 to 1440 minutes, with a CPP amount of 0.05 g, pH 6.2, and a fixed AO concentration of 500 mg L⁻¹.

Figure 8 presents the application of experimental data obtained from kinetic studies to these models. Table 4 provides the nonlinear equations and kinetic parameters corresponding to these models.

Figure 8 shows that the equilibrium time is around 300 minutes. The removal of AO was rapid until the 120th minute, after which it remained constant due to the saturation of active sites.

When comparing the R² values of the kinetic models, it was found that the R² value for PSO is closer to 1, indicating better compatibility of biosorption with PSO. This compatibility with PSO suggests that the removal of AO dye occurs chemically. This chemical process involves electron sharing or exchange between the functional groups of CPP and AO dye molecules [39].

Additionally, the closer results found between the theoretically calculated Qt value using the PSO kinetic model and the experimentally determined Qe value in this biosorption process indicate that PSO is more applicable.

It can be said that the graph of the IPD model in Figure 8, containing two linear components, encompasses the surface and intra-particle diffusion stages of the biosorption process. According to the IPD model, the first linear component indicates that dye molecules quickly adhere to the biosorbent surface, while the second linear component suggests that AO dye molecules diffuse into the pores of the biosorbent. In this case, it can be said that the biosorption kinetic mechanism is compatible with the PSO and IPD kinetic models.

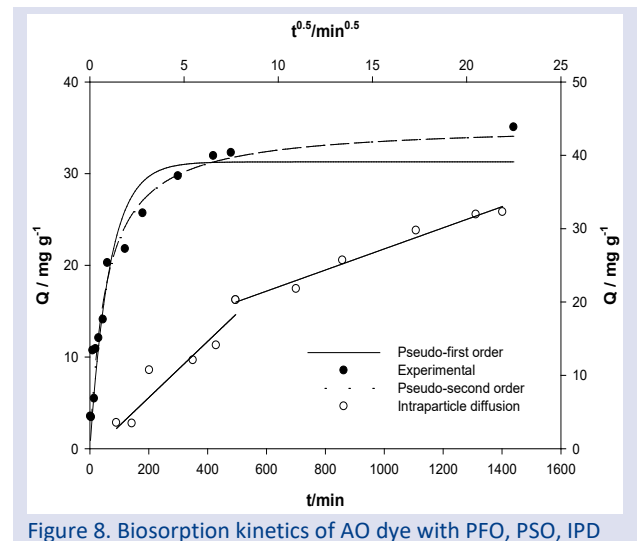


Figure 8. Biosorption kinetics of AO dye with PFO, PSO, IPD

Table 4. Equations and parameters for biosorption kinetic models

Kinetic Models	Equations	Parameters	Values	R ²
PFO	$Q_t = Q_e(1 - e^{-k_1 t})$ $H_1 = k_1 \cdot Q_e$	Q _t (mg/ g) Q _e (mg/ g) k ₁ (g/ mg min) H ₁ (mg/ g min)	31,29 35,06 1,485x 10 ⁻² 46,46 x 10 ⁻²	0,933
PSO	$Q_t = t/[k_2 \cdot Q_e^2] + [1/Q_e] \cdot t$ $H_2 = k_2 \cdot Q_e$	Q _t (mg/ g) Q _e (mg/ g) k ₂ (g/ mg min) H ₂ (mg/ g min)	35,38 35,06 2,55 x 10 ⁻⁵ 3,19 x 10 ⁻²	0,965
IPD	$Q_t = k_i \cdot t^{0,5}$	k _i (mg/ g min ^{0,5})	11,16 x 10 ⁻³	0,976

Biosorption Thermodynamics

Temperature is a crucial factor that influences the diffusion rate through active binding sites on the biosorbent and the solubility of adsorbates in aqueous media [40]. Therefore, thermodynamic studies were conducted at various temperatures, including 278 K, 298 K, and 313 K, to elucidate the impact of temperature on the biosorption of AO dye to CPP. Thermodynamic parameters, such as enthalpy (ΔH° , kJ mol⁻¹), entropy (ΔS° , J mol⁻¹ K⁻¹), and Gibbs free energy (ΔG° , kJ mol⁻¹), were determined using Equation [4-7] [6] and are presented in Table 5.

$$K_d = \frac{Q}{C_e} \tag{4}$$

$$\ln K_D = \frac{\Delta S^\circ}{R} - \frac{\Delta H^\circ}{RT} \tag{5}$$

$$\Delta G^\circ = -RT \ln(K_d) \tag{6}$$

$$\Delta G^\circ = \Delta H^\circ - T\Delta S^\circ \tag{7}$$

The ΔH° and ΔS° values were calculated by determining the slope and intercept of the line obtained from plotting the $1/T$ graph against $\ln K_D$. A positive ΔH° value indicates that the biosorption of AO dye onto CPP increases with temperature, suggesting an endothermic nature. ΔH° value of less than 20 kJ mol⁻¹ suggests that the biosorption is occurring physically. The positive value of ΔS° indicates an increase in randomness and irregularity at the interface of CPP and AO dye solution during the biosorption process. The negative value of ΔG° at increasing temperatures indicates that the biosorption process occurs spontaneously.

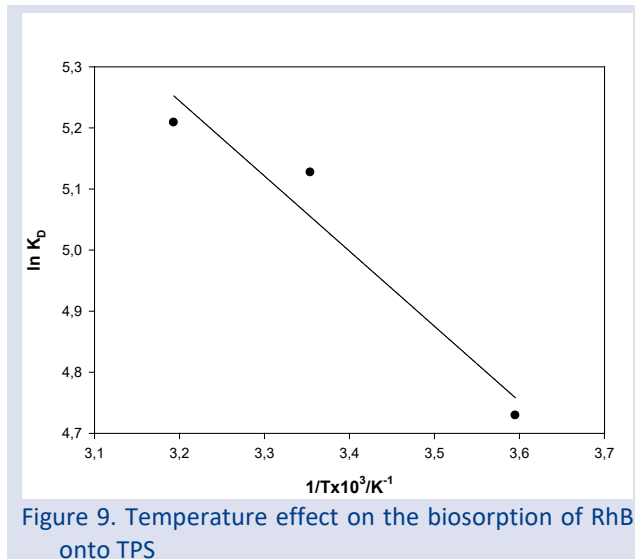


Figure 9. Temperature effect on the biosorption of RhB onto TPS

Table 5. Thermodynamic parameters

Temperature	ΔH	ΔG	ΔS	R^2
278		-14,174		
298	10,226	-15,924	76,31	0,939
313		-17,24		

Recovery

Recovery of AO molecules bound to the CPP surface is one of the most important steps determining the cost of the biosorption process. Therefore, recovery studies of AO molecules from CPP were carried out using 0.1 M HCl, ethanol and methanol solutions. As shown in Figure 10, the recovery percentages were determined as 61%, 72% and 64% for HCl, ethanol and methanol, respectively. According to these results, CPP can be considered as a promising biosorbent for the recovery of AO dye molecules.

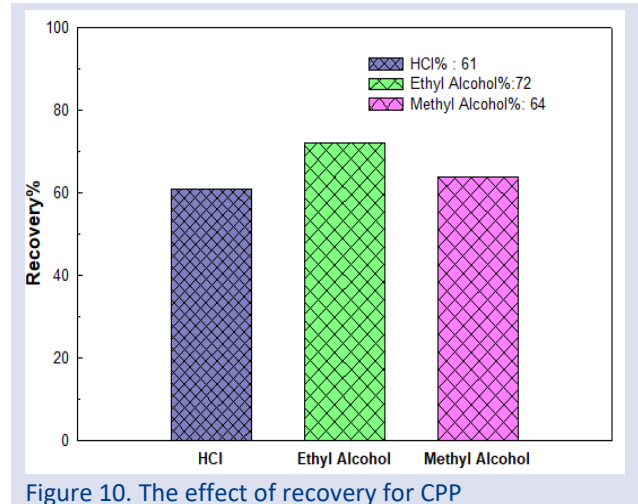


Figure 10. The effect of recovery for CPP

Conclusion

Batch adsorption experiments were conducted to investigate the potential of CPP, a sustainable and renewable agricultural waste, as a biosorbent for the removal of AO dye from aqueous solutions. The objective of this study is to investigate the influence of various operational factors on biosorption. These factors include solution pH, initial AO concentration, zero charge point, CPP quantity, temperature, and contact duration. The morphological structure and functional compounds of the CPP biosorbent were analyzed using FTIR, SEM, EDX and BET characterization techniques. In biosorption isotherm studies, the experimental data were assessed using Langmuir, Freundlich, and D-R isotherm models. The evaluation revealed that the biosorption process aligned with the Langmuir isotherm model, as indicated by its higher correlation coefficient. According to the Langmuir model, the maximum biosorption capacity of the monolayer was calculated to be 177.96 mg/g at 25 °C and pH 6.2. The E_{DR} value calculated from the D-R isotherm model is 7.128 kJ/mol, indicating that the biosorption process is progressing physically. The kinetic study of AO biosorption on CPP showed that PSO is better suited to the biosorption kinetic mechanism. The thermodynamic analysis indicates that the biosorption process is endothermic ($\Delta H^\circ > 0$) and spontaneous ($\Delta S^\circ > 0$). Furthermore, it has been found that the irregularity at the interface between the biosorbent and dye solution (where $\Delta G^\circ < 0$) increases as the biosorption process progresses. The study results show that the CPP

biosorbent, an agricultural waste with minimal cost, can effectively remove AO dye from aqueous media.

Conflicts of interest

The authors declare that, there are no conflicts of interest in this work.

References

- [1] Boukarma L, Aboussabek A, El Aroussi F, Zerbet M, Sinan F, Chiban M., Insight into mechanism, Box-Behnken design, and artificial neural network of cationic dye biosorption by marine macroalgae *Fucus spiralis*, *Algal. Res.*, 76 (2023) 103324.
- [2] Akindolie M.S, Choi H.J., Acid modification of lignocellulosic derived material for dye and heavy metals removal: A review, *Environ Eng Res.*, 28 (2023) 0–3. Gajipara Y.N, Balpande D.N., Patil P.S., Yadav A.A., Yadav M.D., Patwardhan A.V., Jackfruit Leaf-Based Natural Adsorbent for the Efficient Removal of Auramine O Dye, *Water Conserv. Sci. Eng.*, 8 (2023) 1–13.
- [3] Mahajan P, Jaspal D, Malviya A., Adsorption of dyes using custard apple and wood apple waste: A review, *J. Indian Chem. Soc.*, 100 (2023) 100948.
- [4] Sánchez-Ponce L., Díaz-de-Alba M., Casanueva-Marengo M.J., Gestoso-Rojas J., Ortega-Iguña M., Galindo-Riaño M.D., et al, Potential Use of Low-Cost Agri-Food Waste as Biosorbents for the Removal of Cd(II), Co(II), Ni(II) and Pb(II) from Aqueous Solutions, *Separations*, 9(10) (2022) 309.
- [5] Hambisa A.A., Regasa M.B., Ejigu H.G., Senbeto C.B., Adsorption studies of methyl orange dye removal from aqueous solution using Anchote peel-based agricultural waste adsorbent, *Appl. Water Sci.*, 13(24) (2023) 1–11.
- [6] Kainth S., Sharma P., Panney O.P., Green sorbents from agricultural wastes: A review of sustainable adsorption materials, *Applied Surface Science Advances*, 19 (2024) 100562.
- [7] Hadadi A., Imessaoudene A., Bollinger J.C., Cheikh S., Manseri A., Mouni L., Dual Valorization of Potato Peel (*Solanum tuberosum*) as a Versatile and Sustainable Agricultural Waste in Both Bioflocculation of Eriochrome Black T and Biosorption of Methylene Blue., *J. Polym Environ.*, 31 (2023) 2983–98.
- [8] Kumari S., Verma A., Sharma P., Agarwal S., Rajput V.D., Minkina T., et al., Introducing machine learning model to response surface methodology for biosorption of methylene blue dye using *Triticum aestivum* biomass, *Sci. Rep.*, 13 (2023) 8574.
- [9] Handayani T., Emriadi, Deswati, Ramadhani P., Zein R., Modelling studies of methylene blue dye removal using activated corn husk waste: Isotherm, kinetic and thermodynamic evaluation, *South African J. Chem. Eng.*, 47 (2024) 15–27.
- [10] Naboulsi A., Naboulsi I., Regti A., El Himri M., El Haddad M., The valorization of rosemary waste as a new biosorbent to eliminate the rhodamine B dye, *Microchem. J.*, 191 (2023) 108790.
- [11] Ouettar L., Guechi E.K., Hamdaoui O., Fertikh N., Saoudi F., Alghyamah A., Biosorption of Triphenyl Methane Dyes (Malachite Green and Crystal Violet) from Aqueous Media by Alfa (*Stipa tenacissima* L.) Leaf Powder, *Molecules*, 28(8) (2023) 3313.
- [12] Zhang Y., Huang X., Zeng X., Li L., Jiang Y., Preparation, functional properties, and nutritional evaluation of chickpea protein concentrate, *Cereal Chem.*, 100 (2023) 310–20.
- [13] Keskin Z.S., Efficient adsorption of Pb(II) ions using novel adsorbent polyacrylamide/coffee ground composite: isotherm, kinetic and thermodynamic studies, *Polym. Bull.*, (2023). <https://doi.org/10.1007/s00289-023-05111-x>
- [14] Isik B., Avci S., Cakar F., Cankurtaran O., Adsorptive removal of hazardous dye (crystal violet) using bay leaves (*Laurus nobilis* L.): surface characterization, batch adsorption studies, and statistical analysis, *Environ Sci. Pollut. Res.*, 30 (2023) 1333–56.
- [15] Choong Lek B.L., Peter A.P., Qi Chong K.H., Ragu P., Sethu V., Selvarajoo A., et al., Treatment of palm oil mill effluent (POME) using chickpea (*Cicer arietinum*) as a natural coagulant and flocculant: Evaluation, process optimization and characterization of chickpea powder, *J. Environ. Chem. Eng.*, 6 (2018) 6243–55.
- [16] Petrović M., Šošćarić T., Stojanović M., Milojković J., Mihajlović M., Stanojević M., et al., Removal of Pb²⁺ ions by raw corn silk (*Zea mays* L.) as a novel biosorbent, *J. Taiwan Inst. Chem. Eng.*, 58 (2016) 407–16.
- [17] Fatombi J.K., Lartiges B., Aminou T., Barres O., Caillet C., A natural coagulant protein from copra (*Cocos nucifera*): Isolation, characterization, and potential for water purification, *Sep Purif Technol.*, 116 (2013) 35–40.
- [18] Garg U., Kaur M.P., Jawa G.K., Sud D., Garg V.K., Removal of cadmium (II) from aqueous solutions by adsorption on agricultural waste biomass, *J. Hazard Mater.*, 154 (2008) 1149–57.
- [19] Mansour R.A., El Shahawy A., Attia A., Beheary M.S., Brilliant Green Dye Biosorption Using Activated Carbon Derived from Guava Tree Wood, *Int. J. Chem. Eng.*, 2020 (2020) 8053828.
- [20] Şenol Z.M., Keskin Z.S., Şimşek S., Synthesis and characterization of a new hybrid polymer composite (pollene@polyacrylamide) and its applicability in uranyl ions adsorption, *J. Radioanal Nucl. Chem.*, 332 (2023) 2239–2248.
- [21] Hevira L, Zilfa, Rahmayeni, Ighalo J.O., Zein R., Biosorption of indigo carmine from aqueous solution by Terminalia Catappa shell, *J. Environ. Chem. Eng.*, 8 (2020)104290.
- [22] Akkari I., Graba Z., Bezzi N., Merzeg F.A., Bait N., Ferhati A., Raw pomegranate peel as promise efficient biosorbent for the removal of Basic Red 46 dye: equilibrium, kinetic, and thermodynamic studies, *Biomass Convers Biorefinery*, 13 (2023) 8047–60.
- [23] Amar I.A., Biosorption Removal of Methylene Blue Dye from Aqueous Solutions using Phosphoric Acid-Treated Balanites Aegyptiaca Seed Husks Powder, *Biointerface Research in Applied Chemistry*, 12(6) (2022) 7845–62.
- [24] Al-Asadi S.T., Al-Qaim F.F., Al-Saedi H.F.S., Deyab I.F., Kamyab H., Chelliapan S., Adsorption of methylene blue dye from aqueous solution using low-cost adsorbent: kinetic, isotherm adsorption, and thermodynamic studies, *Environ Monit Assess*, 195 (2023) 676.
- [25] Ayawei N., Ebelegi A.N., Wankasi D., Modelling and Interpretation of Adsorption Isotherms, *J Chem.*, 2017 (2017) 3039817.
- [26] Şenol Z.M., Gül Ü.D., Şimşek S., Bioremoval of Safranin O dye by the identified lichen species called *Evernia prunastri* biomass; biosorption optimization, isotherms, kinetics, and thermodynamics, *Biomass Convers Biorefinery.*, 12 (2022) 4127–37.
- [27] Mohammed R.A., Walli H.A., A Study of Removal of Lead (II) Ions from Aqueous Solution on Chitosan-g-poly (acrylic acid-co-crotonic acid) Hydrogel, *Int J Drug Deliv Technol.*, 12 (2022) 1844–8.
- [28] Keskin Z.S., Şenol Z.M., Kaya S., Şimşek S., Prunus mahaleb shell as a sustainable bioresource for carminic acid removal from aqueous solution: Experimental and theoretical studies, *J. Mol. Struct.*, 1275 (2023) 134618.
- [29] Al-Ghouthi M.A., Da'ana D.A., Guidelines for the use and interpretation of adsorption isotherm models: A review, *J. Hazard Mater.*, 393 (2020) 122383.
- [30] Dada A.O., Adekola F.A., Odeunmi E.O., Dada F.E., Bello O.M., Akinyemi B.A., et al., Sustainable and low-cost *Ocimum gratissimum* for biosorption of indigo carmine dye: kinetics, isotherm, and thermodynamic studies, *Int. J.*

- Phytoremediation*, 22 (2020) 1524–37.
- [31] Şenol Z.M., Çetinkaya S., Yenidünya A.F., Başoğlu-Ünal F., Ece A., Epichlorohydrin and tripolyphosphate-crosslinked chitosan–kaolin composite for Auramine O dye removal from aqueous solutions: Experimental study and DFT calculations, *Int. J. Biol. Macromol.*, 199 (2022) 318–30.
- [32] Sözüdoğru O., Investigation of Effective Removal of Auramine O Dye by *Pyracantha Coccinea* Biosorbent: Isotherm and Kinetics, *Brill Eng.*, 4 (2023) 1–6.
- [33] Vaid V., Jindal R., Biodegradable tamarind kernel powder/kappa-carrageenan hydrogel for efficient removal of cationic dyes from effluents, *Water Environ. Res.*, 95 (2023) 1–21.
- [34] Shakeri S., Rafiee Z., Dashtian K., Fe₃O₄-Based Melamine-Rich Covalent Organic Polymer for Simultaneous Removal of Auramine O and Rhodamine B., *J. Chem. Eng. Data*, 65 (2020) 696–705.
- [35] Duarte E.D.V., Vieira W.T., Góes R.O., de Azevedo L.E.C., Vieira M.G.A., da Silva M.G.C., et al., Amazon raw clay as a precursor of a clay-based adsorbent: experimental study and DFT analysis for the adsorption of Basic Yellow 2 dye, *Environ. Sci. Pollut. Res.*, 30 (2023) 62602–24. A
- [36] Şenol Z.M., Şimşek S, Equilibrium, kinetics and thermodynamics of Pb(II) ions from aqueous solution by adsorption onto chitosan-dolomite composite beads, *Int. J. Environ. Anal. Chem.*, 102(17) (2022) 4926–40.
- [37] Thompson C.O., Ndukwe A.O., Asadu C.O., Application of activated biomass waste as an adsorbent for the removal of lead (II) ion from wastewater, *Emerg Contam.*, 6 (2020) 259–67.
- [38] Şenol Z.M, El Messaoudi N., Fernine Y., Keskin Z.S., Bioremoval of rhodamine B dye from aqueous solution by using agricultural solid waste (almond shell): experimental and DFT modeling studies, *Biomass Convers Biorefinery*, (2023) <https://doi.org/10.1007/s13399-023-03781-1>.
- [39] Zafar L., Khan A., Kamran U., Park S., Nawaz H., Eucalyptus (*camaldulensis*) bark-based composites for efficient Basic Blue 41 dye biosorption from aqueous stream : Kinetics , isothermal , and thermodynamic studies, *Surfaces and Interfaces* , 31 (2022) 101897.